DOI: 10.1002/ejic.201001216

Discrete Molecular Squares $\{[(en)M(CN)]_4\}^{4+}$ Derived from $[(en)M(CN)_2]$ ($M = Pt^{II}, Pd^{II}$)

Anzhela Galstyan,[a] Pablo J. Sanz Miguel,[a,b] Jacqueline Wolf,[a] Eva Freisinger,[c] and Bernhard Lippert*[a]

Keywords: Cyanides / Platinum / Palladium / Metallacycles / Model nucleobases

C_{2h}-symmetrical tetranuclear metallacycles $\{[M(en)(CN)]_4\}(NO_3)_4$ with $M = Pd^{II}$ (**4**) and Pt^{II} (**5**) have been prepared upon reacting $M(en)(CN)_2$ [$M = Pd^{II}$ (**1**), Pt^{II} (**2**)] with $[M(en)(H_2O)_2](NO_3)_2$. Replacement of the nitrate anions of **5** by terephthalate anions yields the corresponding salt **5a**. The X-ray crystal structures of **1**, **4**, **5**, and **5a** have been determined. In the metallacycles **4**, **5**, and **5a** the four metals form almost ideal squares with average M···M distances of ca. 5.05 Å (**5**, **5a**) and 5.08 Å (**4**) along the sides. As shown by ^1H NMR spectroscopy, the Pt square **5** is stable in aqueous solution, whereas the Pd square **4** undergoes rearrangement reactions upon aging or the presence of other Pd species such as (bpy)Pd^{II}. Preliminary studies on the possibility of non-covalent interactions of **4** and **5** with model nucleobases in water reveal that only **5** is useful in this respect. According to the concentration-dependence ^1H NMR study, there is an interaction with the purine base 9-ethyladenine, molecular details of which are unclear at this stage, however. Compound **4** is substitutionally labile and is transformed into the coordination compound **8** with 1-methylcytosine. Two more side products, produced during the various reactions carried out, were characterized by X-ray crystallography: $[Pt(en)_2][Pt(CN)_4]$ (**3**) and $[Pd(bpy)(en)](SO_4)\cdot 3H_2O$ (**7**).

Introduction

Cyanide is an extremely versatile ligand in coordination chemistry, binding to transition metal ions in numerous ways such as monofunctional (via C or N), bifunctional (via C and N or via C and π bond), or even trifunctional (via C and two π bonds) manners.[1] It is widely applied for the construction of coordination polymers,[2] but when combined with capping ligands, discrete 3D- and 2D-coordination compounds with bridging cyanide ligands can be generated.[3,4] The interest in magnetic properties of large clusters and the hope of generating novel molecule-based magnets are major driving forces for research.

Our interest in the topic of μ-CN^--bridged complexes relates to our ongoing efforts to generate discrete molecular architectures from metal entities and heterocyclic ligands, including nucleobases, in general,[5] and from our attempts to produce (essentially) flat constructs,[6] which are kinetically robust and have the potential of interacting with so called guanine quartets (G_4). The latter occur in tetra-stranded DNA ("quadruplex DNA") which in turn is part of the telomeres at the end of the chromosomes, and also can be formed in the promoter region of the genes.[7] Tetra-

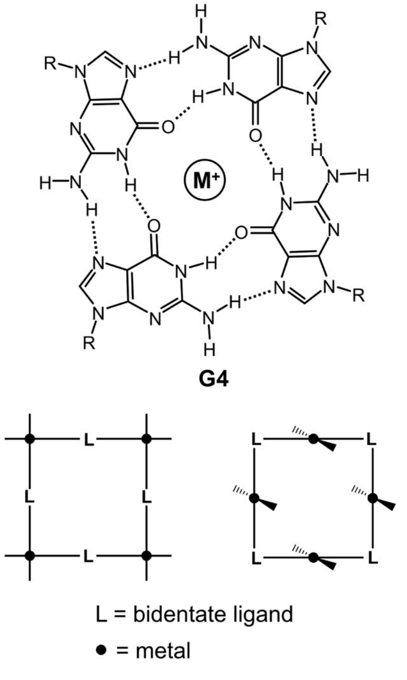

Figure 1. Schematic views of guanine quartet (G_4) (top) and of discrete molecular squares with *cis*-a_2M^{II} (bottom, left) and *trans*-a_2M^{II} (with M = Pt or Pd) (bottom, right).

---

[a] Fakultät Chemie, Technische Universität Dortmund,
44221 Dortmund, Germany
Fax: +49-231-755-3769
E-mail: bernhard.lippert@tu-dortmund.de
[b] Departamento de Química Inorgánica, Instituto Universitario de Catálisis Homogénea, Instituto de Ciencia de Materiales de Aragón, Universidad de Zaragoza – C.S.I.C.
50009 Zaragoza, Spain
[c] Institute of Inorganic Chemistry, University of Zürich,
8057 Zürich, Switzerland

Supporting information for this article is available on the WWW under http://dx.doi.org/10.1002/ejic.201001216.

stranded DNA regions have become a major focus as a novel target in anticancer chemotherapeutic approaches in recent years.[8] In brief, any stabilization of quadruplex DNA, either in telomeres or in gene-regulatory elements, for instance through π-π stacking by an organic ligand[9] or a suitable metal compound,[10] appears to be advantageous in terms of tumor suppression.

The focus of our work is thus on complexes having a *cis*-a_2M^{II} (M = Pt or Pd; a = NH_3 or a_2 = chelating diamine) in the corner of a square, or a corresponding *trans*-a_2M^{II} (M = Pt or Pd; a = NH_3 or monodentate amine) in the center of the side of a square (Figure 1).

Here we report on the synthesis and characterization of cyanido-bridged complexes of Pt^{II} and Pd^{II}, with the metals residing in the corners of the squares.

Results and Discussion

General Aspects

Spontaneous self-assembly of *cis*-a_2M^{II} entity with CN^- to a molecular square can lead, in principle, to four different linkage isomers **I**–**IV** (Figure 2).

Formation of **I** feasibly could take place in a cyclization reaction of four mononuclear *cis*-$a_2M(CN)^+$ cations, while **II** and **III** could be formed upon condensation of a neutral bis(cyanide) complex *cis*-$a_2M(CN)_2$ with two mononuclear *cis*-$a_2M(CN)^+$ cations and a *cis*-a_2M^{2+}. Finally **IV** could arrange from two neutral *cis*-$a_2M(CN)_2$ molecules and two *cis*-a_2M^{2+}. In all cases it is assumed that initial coordination of CN^- to M is through the carbon atom. Moreover, this view implies that no ligand scrambling occurs during synthesis.

Although for the tetrameric $[Me_2Au(CN)]_4$ (Me = methyl) a type-**I** isomer has been postulated, ^1H NMR spectroscopy suggests the presence of disordered CN^- ligands.[11] X-ray crystal structures of cyclic CN-bridged Pt^{II} compounds are scarce and reveal both disordered[12a] and ordered CN^- bridges.[12b,12c] A further potential complication arises from the possibility of equilibria between squares and triangles. Although relatively rare,[13] CN^--bridged metallacycles have been reported and represent an entropically favored alternative to molecular squares. Attempts to prepare μ-CN compounds by reaction of $[(en)M(H_2O)_2]^{2+}$ with 1 equiv. of CN^- failed in that mixtures of compounds were obtained, according to ^1H NMR spectroscopy (see below). In order to reduce the number of possible species, a "directed" approach[14] was undertaken to obtain type-**IV** compounds by starting from $(en)M(CN)_2$ and reacting it subsequently with $[(en)M(H_2O)_2]^{2+}$ (M = Pt^{II} and/or Pd^{II}). This strategy eventually led to Pt_4 and Pd_4 species. Previously reported examples of CN^--bridged mixed Fe_2Co_2[3b] and mixed Fe_2Cu_2[3c] squares were synthesized applying the same approach.

Concerning the use of ^1H NMR spectroscopy to study (en)M complexes, it was anticipated that binding of CN^- via C *or* binding via N should affect the CH_2 protons of the en chelate ring differently. Consistent with this view, a single CH_2 resonance is to be expected for $(en)M(CN)_2$, whereas a mixed coordination (en)M(*C*N)(*N*C) or the simultaneous existence of $(en)M(CN)_2$ and $(en)M(NC)_2$ should give rise to two sets of CH_2 resonances. It was unclear, however, whether the four possible cyclic structures **I**–**IV**, could be differentiated by this method in case of four identical metals (e.g., M = Pt^{II} or Pd^{II}), as there are four M–C and four M–N bonds in each structure. For en ligands bonded to Pt, ^3J coupling between methylene protons and the ^{195}Pt isotope was considered helpful. As another means of differentiating terminal and bridging CN^- ligands, IR spectroscopy was applied.[15] This method relies on differences in the position of the ν(CN) stretching modes, which occur at significantly higher wavenumbers when CN^- acts as bridge.

X-ray Crystal Structures of the Starting Complex, of a Side Product and of Two Squares

Of the two building blocks with a *cis* geometry, $Pd(en)(CN)_2$ (**1**) and $Pt(en)(CN)_2$ (**2**), only the Pd compound was obtained as crystals suitable for X-ray diffraction (Figure 3). In **1** Pd adopts a square-planar geometry,

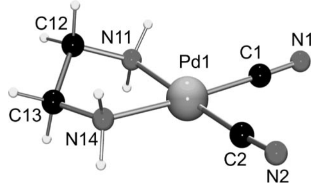

Figure 3. View of $Pd(en)(CN)_2$ (**1**) with atom numbering scheme.

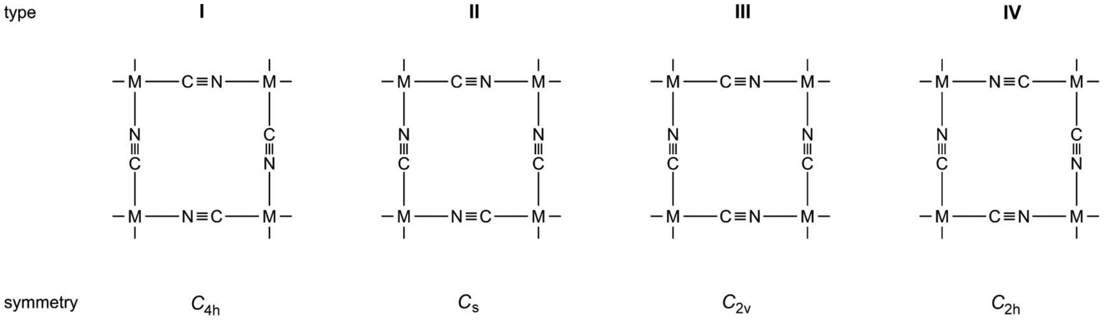

Figure 2. Four possible linkage isomers of cyclic, tetranuclear *cis*-$\{[a_2M(CN)]_4\}^{4+}$ species and their respective symmetries.

containing a chelating ethylendiamine ligand and two terminal cyanido ligands.

Distances and angles about the Pd are normal, as are the geometries of the en and cyanide ligands (Supporting Information). The crystal packing of **1** is dominated by hydrogen bonding, involving nitrogen acceptor (CN^-) and donor (NH_2) groups. No electrostatic or metal-metal interactions are observed. An almost right dihedral angle (89.5°) is formed between the PtC_2N_2 coordination planes of two neighboring molecules of **1**, which are twofold H-bonded: N1···(H)N14, 3.038(3) Å; N2···(H)N14, 3.084(3) Å. Further related twofold hydrogen bonds allow the formation of zigzag chains along the *c* axis. The distance between Pd atoms within a chain is 5.3122(2) Å. Antiparallel chains are connected by hydrogen bonds: N1···(H)N14, 2.991(3) Å; N2···(H)N14, 3.101(3) Å.

The analogous Pt complex, $Pt(en)(CN)_2$ (**2**) was not obtained in monocrystalline form, but its formation was concluded from ^1H NMR spectra (see below). However, a side product which proved to be $[Pt(en)_2][Pt(CN)_4]$ (**3**), was isolated in low yield and characterized by X-ray analysis (Figure 4). Compound **3** crystallizes in a way reminiscent of Magnus' green salt,[16] hence has a chain structure with alternating $[Pt(en)_2]^{2+}$ cations and $[Pt(CN)_4]^{2-}$ anions. However, Pt–Pt distances within the chain are markedly different, 3.3205(14) Å and 4.0106(14) Å, and therefore a more appropriate description might be that of weakly interacting cation-anion pairs. The polymeric chains are oriented along the *b* axis and interconnected by hydrogen bonds between NH_2 groups of en ligands and N atoms of the terminal CN^- ligands [N4···N21, 2.99(4) Å; N6···N24, 2.99(4) Å]. Neighboring chains also interact via H-bonding: N2···N11, 2.97(4) Å; N2···N24, 3.01(3) Å; N8···N14, 2.90(4) Å.

Reactions of **1** and **2**, respectively, with one equivalent of $[M(en)(H_2O)_2](NO_3)_2$ produce the designed squares of composition $\{[Pd(en)(CN)]_4\}(NO_3)_4$ (**4**) and $\{[Pt(en)(CN)]_4\}(NO_3)_4$ (**5**). Both compounds were X-ray structurally characterized, and both crystallize in space group $P\bar{1}$ with almost identical volumes of the unit cells. Both cations are therefore virtually analogous and only the cation of **5** is depicted in Figure 5. The refinements of both structures are consistent with the presence of linkage isomer **IV**. Upon sequential inversion of C and N sites, larger *R* values and thermal parameters outside the range of average parameters for the structure were obtained.

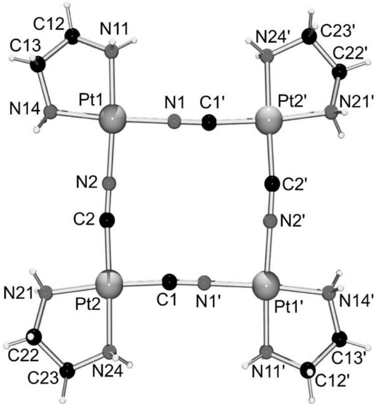

Figure 5. View of the symmetry-generated cation of $\{[Pt(en)(CN)_4]\}(NO_3)_4$ (**5**). The corresponding cation with Pd instead of Pt (**4**) is very similar and not shown.

Salient structural features (given for **5** only, for **4** see Supporting Information) are as follows: two of the four Pt atoms are bonded to C atoms of the CN^- bridges, while the two others are bonded to the N atoms of CN^-. Pt–C and Pt–N distances are Pt1–N1, 1.978(10) Å; Pt1–N2, 2.000(13) Å; Pt2–C1, 1.986(10) Å; Pt2–C2, 1.945(12) Å. Pt–Pt distances along the sides of the molecular square are 5.0413(7) Å (Pt1–Pt2) and 5.0661(7) Å (Pt1–Pt2′) and the diagonals are 7.1008(7) Å (Pt1–Pt1′) and 7.1938(8) Å (Pt2–Pt2′). Although **4** and **5** are analogous, there are differences in the solid state packing. Both complexes form stairs by stacking of opposite corners of the squares with adjacent squares (**4** along the *a* axis, **5** along the *b* axis). Distances between adjacent stacked squares (plane-centroid) are significantly different, ca. 3.5 Å for **4**, and 3.8 Å for **5** (Figure 6). In addition, the geometrical projection of the atoms of a square in the plane of its neighbor also differs in **4** and **5**. In the case of **4**, two (en)Pd groups of the previous and next squares of the stair are projected within the square. The inside part of the square **5** includes the projection of a part (two carbon and one nitrogen atoms) of two en groups, resulting thus in a partially twisted stair. An inspection of the packing patterns further reveals that stair formation in **4** and **5** is largely a consequence of hydrogen bonding between the NH_2 groups of the en ligands and nitrate anions (roughly in the plane of the cations) as well as water mole-

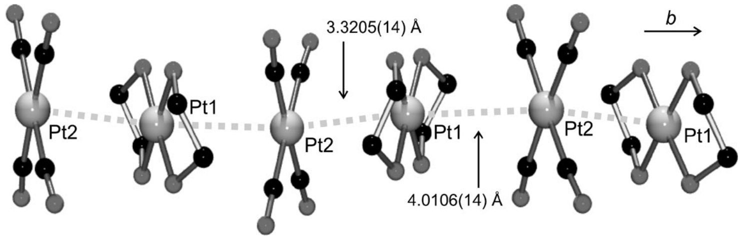

Figure 4. Section of chain structure of alternating pairs of cations and anions in $[Pt(en)_2][Pt(CN)_4]$ (**3**).

cules (both in the plane of the cations and between the cation sheets). Vertical Pd···Pd [3.5375(10) Å, **4**] and Pt···Pt [3.5699(11) Å, **5**] interactions may add to the packing.

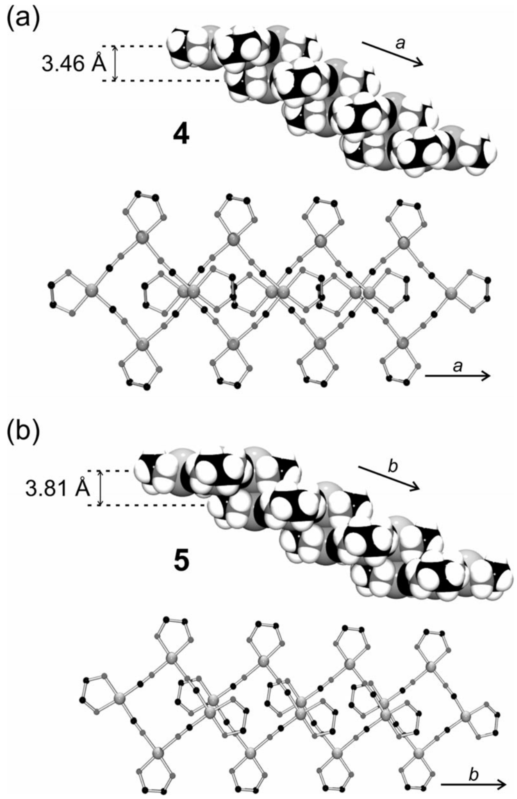

Figure 6. Different crystal packing of cations **4** and **5**.

Anion Exchange with 5

In order to screen for any striking host-guest interactions of cation **5** with selected anions, aqueous solutions of **5** were treated with increasing amounts of NaF, NaCl, Na_2SO_4, and the disodium salt of terephthalate, and changes in chemical shifts of the two methylene signals of en were monitored by ^1H NMR spectroscopy. For all anions, smooth downfield shifts were observed, however, they did not exceed $\Delta\delta$ values of 0.1 ppm even when present in high excess (> 50 fold; [**5**] = 8×10^{-3} M). The weak response of both en resonances to the added anions suggests only weak anion binding and was therefore not further investigated. From the NMR sample with terephthalate, crystals were obtained, which were studied by X-ray crystallography and revealed a composition of $\{[Pt(en)(CN)]_4\}(C_8H_4O_4)_2 \cdot 10H_2O$ (**5a**). A view of **5a** is given in Figure 7.

Cation **5a** shows in essence a very similar geometry as **4**. Pt–C and Pt–N distances within the square are Pt1–N1, 1.966(12) Å, Pt1–N2, 1.948(12) Å, Pt2–C1, 1.937(14) Å and Pt2–C2, 1.923(15) Å. Likewise, the packing of cations **5a** corresponds to that of **4**, forming stairs (in this case along the *a* axis) with projections of the neighbor (en)Pt entities within the square of **5a**; the distance Pt2–Pt2 of two stacked cations is 3.4334(11) Å. Terephthalate anions are placed between stairs of **5a**, interacting through hydrogen bonds with water molecules and cations (Supporting Information).

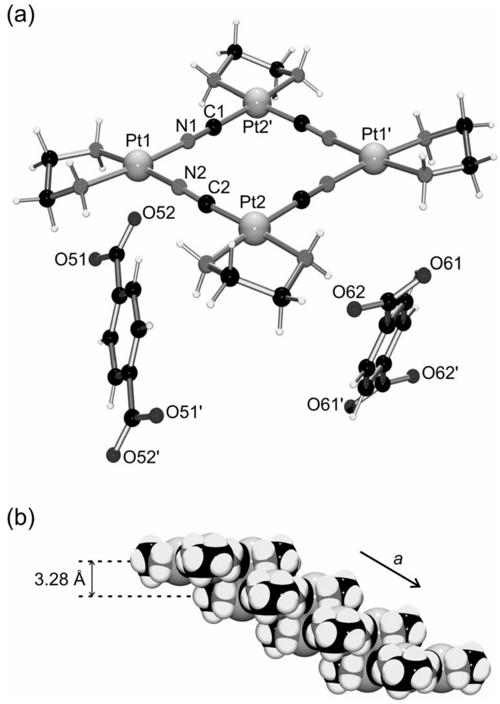

Figure 7. View of cation and anions of **5a**.

IR and NMR Spectroscopy

As the wavenumbers of the CN stretching vibrations are known to be indicative of the coordination mode of the cyanide ligands, IR spectra were recorded. Wavenumbers of the υ(CN) absorption bands are listed in Table 1. They are close to expectations for terminal and bridging CN^- ligands, with the latter usually occurring at significantly higher wavenumbers.[15]

Table 1. Vibrational frequencies of υ(CN) in the various compounds.

	1	3	4	5	6
υ(CN) [cm^{-1}]	2145, 2135	2123	2190	2192	2190

As mentioned above, reactions of $Pt(en)Cl_2$ with 1 equiv. of $AgNO_3$ and 1 equiv. of AgCN, hence with a Pt/CN^- ratio of 1:1, give a ^1H NMR spectrum with multiple CH_2 resonances between 2.46 and 2.78 ppm. In contrast, both $Pt(en)(CN)_2$ (**2**) (δ = 2.65 ppm) and $[Pt(en)_2][Pt(CN)_4]$ (**3**) (δ = 2.78 ppm) display singlets with ^{195}Pt satellites due to ^3J coupling (40 Hz in **2**, 32 Hz in **3**), whereas the cyclic tetramer **5** has two singlets of identical intensities at δ = 2.54 and 2.71 ppm (Figure 8). Both resonances reveal ^{195}Pt satellites of ca. 36 Hz and 29 Hz, respectively. We tentatively assignment the two methylene proton signals to Pt(en)(*N*C)$_2$ and Pt(en)(*C*N)$_2$ on the basis of their different $^4J(^{195}Pt\text{-}^1H)$ coupling constants and expectations based on the *trans*-influence concept.[17]

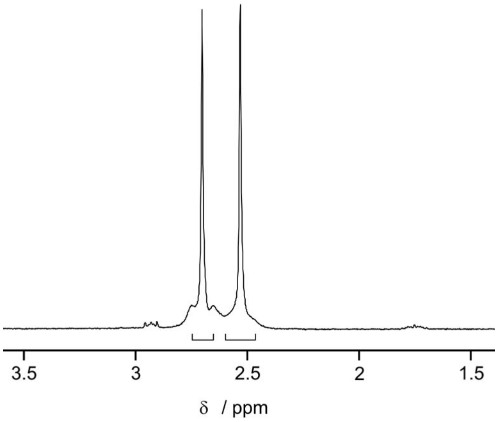

Figure 8. CH_2 resonances of en ligands in $\{[Pt(en)(CN)]_4\}(NO_3)_4$ (**5**) with ^{195}Pt satellites indicated.

^1H NMR spectra (D_2O) of $Pd(en)(CN)_2$ (**1**) and $[Pd(en)(D_2O)_2]^{2+}$ show methylene resonances as singlets at $\delta = 2.80$ and 2.62 ppm, respectively. The ^1H NMR spectrum of a freshly prepared solution of the cyclic tetramer **4**, obtained by dissolving crystals of **4** in D_2O and recording the ^1H NMR spectrum immediately afterwards, shows two CH_2 resonances in 1:1 ratio at $\delta = 2.63$ and 2.75 ppm, similarly to **5**. In contrast to **5**, which does not undergo changes within 3 d at 80 °C, the spectrum of **4** changes with time (Figure 9).

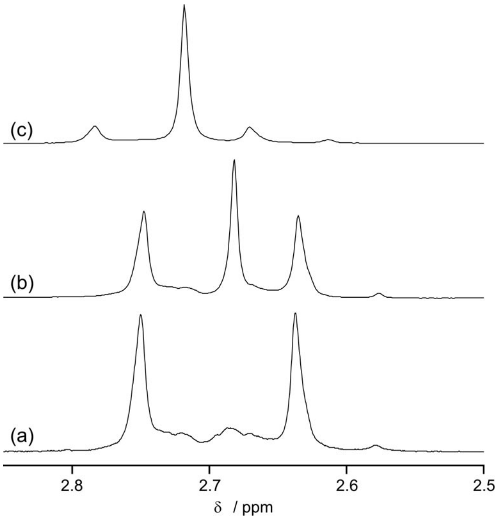

Figure 9. ^1H NMR spectra (D_2O, 300 MHz) of $[Pd(en)(CN)]_4(NO_3)_4$ (**4**) a) immediately after dissolving the crystals, b) after 4 d at room temp. and c) after 1 d at 60 °C.

An aged solution of **4** (3–4 d, r.t.) reveals a new resonance at $\delta = 2.68$ ppm (Figure 9, b), which becomes dominant (and slightly downfield shifted) upon heating (Figure 9, c). Possibly a symmetrisation reaction as shown in Equation (1) could account for this observation, corroborated by our finding on formation of $[Pt(en)_2][Pt(CN)_4]$ (**3**) (see above). Furthermore, we note that the ^1H NMR spectrum of $[Pd(en)_2]^{2+}$, prepared in situ by reaction of $[Pd(en)(D_2O)_2](NO_3)_2$ with en·HCl in D_2O is identical with that given in Figure 9 (c). We rule out the possibility that **4** rearranges into any of the other metallacycles **I**–**III** (Figure 2), as for these species likewise more than a single en resonance would be expected.

Lability of Ligands

Attempts to prepare Pd_4 squares with two kinds of chelating amine ligands at the metals by combining $Pd(en)(CN)_2$ (**1**) with $[Pd(bpy)(H_2O)_2](NO_3)_2$ in water resulted in formation of a gel. When MeOH was applied as the solvent, a white material **6**, insoluble in water and all common organic solvents, was obtained. Compound **6** analyzes as $[Pd_4(bpy)_2(en)_2(CN)_4](NO_3)_4\cdot 2H_2O$ and has a sharp IR band at 2190 cm^{-1}, consistent with the presence of bridging cyanide. The structure of this compound is unknown at present. When this reaction was carried out in more dilute aqueous solution, and with SO_4^{2-} as anion, there was likewise formation of a gel. However, at the same time also a crystalline compound was obtained in 11% yield, which proved to be $[Pd(bpy)(en)](SO_4)\cdot 3H_2O$ (**7**). This finding suggests that amine exchange reactions can occur under the experimental conditions applied. A view of cation **7** is depicted in Figure 10 (a). Cation **7** is planar, except for the carbon atoms of the en group, which are located slightly above and below the plane. Distances and angles within the cation are normal, with deviations of angles around the palladium atom from 90°: Pd1–N11, 2.011(7) Å; Pd1–N21, 2.018(6) Å; Pd1–N1, 2.021(7) Å; Pd1–N4, 2.027(6) Å; N11–Pd1–N21, 81.3(3)°; N21–Pd1–N1, 97.9(3)°; N11–Pd1–N4 96.9(3)°; N1–Pd1–N4, 84.0(3)°. Cations of **7** display π–π stacking of 2,2′-bipyridine rings along the *b* axis (3.3 Å), and are alternatively disposed with the en ligands pointing in opposite directions. Sulfate anions are inserted between two en ligands via H-bonds (Figure 10, b) and water mole-

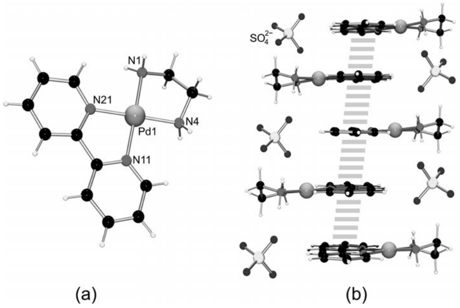

Figure 10. a) View of the cation of **7**, and b) π-stacking of cations, with SO_4^{2-} anions involved in hydrogen bonding.

$$[Pd(en)(CN)]_4(NO_3)_4 \xrightarrow{H_2O} [Pd(en)_2](NO_3)_2 + [Pd(en)_2]\,[Pd(CN)_4] + [Pd(H_2O)_4](NO_3)_2 \qquad (1)$$

cules. Hydrogen bonding distances in the crystal packing of **7** are N1···O1w, 2.86(1) Å, N1···O11, 2.83(1) Å, N4···O12, 2.878(9) Å, N4···O13, 2.913(10) Å, O11···O2w, 2.946(10) Å, O13···O2w, 2.733(9) Å as well as O14···O1w, 2.669(10) Å.

Interactions between Squares and Nucleobases

As a first test of possible interactions of the cationic squares **4** and **5** with nucleobase aggregates (quartets, base pairs) we decided to study the effects on selected model nucleobases on these squares. For this purpose ^{1}H NMR spectra of mixtures of the Pt square **5** with increasing amounts of 1-methylcytosine (1-MeC), 1-methyluracil (1-MeUH) and 9-ethyladenine (9-EtA) were recorded in D_2O. Other bases (9-methylguanine, 1-methylthymine) were not considered because of low solubility. The experiments were carried out at pH values, where no acid-base equilibria are relevant, viz. pD 8.0 ± 0.2 with 1-MeC, 6.8 ± 0.4 with 1-MeUH, and 7.5 ± 0.5 with 9-EtA. With all three nucleobases, increasing concentrations (20–40 fold excess) of the base cause *downfield* shifts of both CH_2 resonances of the en ligands of **5**, but with 9-EtA this effect is almost three times as large as with the two pyrimidine bases, namely between 0.2 and 0.3 ppm. On the other hand, 9-EtA proton resonances, and in particular those of the two aromatic protons H2 and H8, undergo *upfield* shifts with increasing concentrations. In the concentration range 0.003–0.105 M these shifts are 0.30 ppm for H2, 0.26 ppm for H8, and 0.20 ppm for CH_2 of the ethyl group. CH_3 of the ethyl group is virtually unaffected (Supporting Information). This behavior is indicative of adenine stacking, as expected.[18] The marked difference in behavior of the en resonances of **5** in the presence of 9-EtA strongly suggests that there is an interaction between the cation of **5** and the adenine, the nature of which is unclear at present.

The above mentioned instability of the Pd square **4** was also confirmed in an experiment aimed at cocrystallizing **4** with 1-methylcytosine and its hemiprotonated form, the [1-MeC·1-MeCH]$^+$ pair. Upon mixing **4** with [1-MeCH]I, rapid decomposition of **4** and formation of *trans*-[PdI_2(CN)(1-MeC)]$^-$ took place, forming a salt with the hemiprotonated 1-MeC base pair, hence [1-MeC·1-MeCH]-[PdI_2(CN)(1-MeC)]·$2H_2O$ (**8**). The compound is depicted in Figure 11.

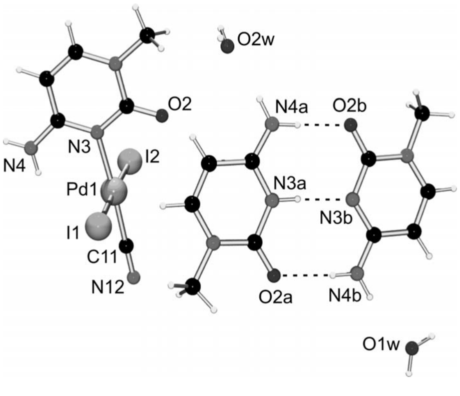

Figure 11. View of [1-MeC·1-MeCH][PdI_2(CN)(1-MeC)]·$2H_2O$ (**8**).

The pyrimidine nucleobase 1-MeC is bonded to Pd^{II} through its N3 site, as is typical for the large majority of metal complexes of N1 substituted cytosine ligands.[19] The geometry of the complex anion is normal as far as bond lengths and angles are concerned (Supporting Information). The 1-MeC ring is almost perpendicular to the Pd coordination plane (83.1°), very much as in the related *trans*-PtI_2(1-MeC) fragment.[20] The cation of **8** reveals the typical geometry of hemiprotonated cytosine bases, which have been crystallized with numerous other counter anions.[21] Formation of the anion of **8** further confirms that the chelating en ligand in Pd^{II} complexes is labile and is prone to substitution by the other ligands, here by I$^-$ and even 1-MeC.

There is no rapid reaction of the Pt square **5** with [1-MeCH]I, but within days at room temperature there is formation of a small amount of a poorly soluble precipitate having an orange color. We believe that it is due to a Pt-iodide species. Still, the ^{1}H NMR spectrum is virtually unaltered (no new H5, H6 doublets of 1-MeC detectable).

Conclusions

Two CN$^-$-bridged molecular squares of (en)Pd^{II} (**4**) and (en)Pt^{II} (**5**) have been obtained with the aim to further study them with regard to their propensity to interact non-covalently with nucleobases, and preferably with guanine quartets or nucleobase aggregates in general. The Pd square proved not to be useful as it was unstable in solution, even in the absence of nucleobases. In contrast, the Pt square **5** is considerably more inert and consequently is more suitable in terms of its potential to interact non-covalently with nucleobases. With the model nucleobase 9-EtA a distinct effect on **5** is seen, but details of this interaction are elusive.

Experimental Section

General: The complexes en$PdCl_2$[22] and en$PtCl_2$[23] were prepared from $K_2[PdCl_4]$ and $K_2[PtCl_4]$ (Heraeus) by literature methods. The model nucleobases 1-MeC,[24] 1-MeUH,[25] and 9-EtA[26] were likewise prepared as reported. All other chemicals were of commercial origin and were used without further purification. ^{1}H NMR spectra were recorded in D_2O on Varian Mercury 200 FT NMR and Bruker DPX 300 spectrometers, with TSP used as an internal reference. pD values were determined by use of a glass electrode and addition of 0.4 to the pH-meter reading. IR spectra were recorded on an IR Fourier spectrometer IFS 28 Firma Bruker Optik GmbH from KBr pellets. Elemental analyses were carried out on a Leco CHNS-932 instrument.

enPd(CN)$_2$ (1): A solution of en$PdCl_2$ (237 mg, 1 mmol) and AgCN (268 mg, 2 mmol) in water (40 mL), after 10 min ultrasonic treatment, was stirred in dark at 40 °C for 18 h. AgCl was removed by filtration and the volume of the solution was reduced to 5 mL. Colorless cubic crystals were grown at 4 °C. The yield was 127 mg (58%). $C_4H_8N_4Pd$ (218.55): calcd. C 21.98, H 3.69, N 25.6; found C 22.0, H 3.7, N 25.6. IR (KBr): $\tilde{\nu}$ = 2145, 2135 [υ(CN)]cm^{-1}. ^{1}H NMR (300 MHz, D_2O): δ = 2.80 (s, CH_2) ppm.

enPt(CN)$_2$ (2) and [Pt(en)$_2$][Pt(CN)$_4$] (3): A solution of en$PtCl_2$ (325 mg, 1 mmol) and AgCN (268 mg, 2 mmol) in water (40 mL) was stirred in dark at 40 °C for ca. 28 h. AgCl that had formed was removed by filtration and the solution containing Pt(en)-$(CN)_2$ (**2**) was used directly for the synthesis of **5** (see below). ^1H NMR (300 MHz, D_2O): δ = 2.65 (s, ^3J = 40 Hz, ^{195}Pt-^1H, CH_2) ppm. When the solution was left at room temp. for 2–3 d, white needles of $[Pt(en)_2][Pt(CN)_4]$ (**3**) were isolated in ca. 10% yield. $C_8H_{16}N_8Pt_2 \cdot H_2O$ (584.4): calcd. C 15.19, H 2.87, N 17.72; found C 15.2, H 2.8, N 17.4. IR (KBr): $\tilde{v}$ = 2123 [υ(CN)]cm^{-1}. ^1H NMR (300 MHz, D_2O): δ = 2.78 (s, ^3J = 32 Hz, ^{195}Pt-^{1} H, CH_2) ppm.

$\{[Pd(en)(CN)]_4\}(NO_3)_4$ (4): To a solution of $[enPd(H_2O)_2](NO_3)_2$, obtained by stirring $enPdCl_2$ (237 mg, 1 mmol) and $AgNO_3$ (340 mg, 2 mmol) in water (30 mL) for 2 h at room temp. followed by filtration of AgCl, was added freshly prepared $enPd(CN)_2$ (1 mmol in 50 mL, water). The bright yellow color of the mixture changed immediately to pale yellow. The volume of the solution was then reduced to 5 mL. The product crystallized within several hours at room temp. The yield was 550 mg (54%). $C_{12}H_{32}N_{16}O_{12}Pd_4$ (1018.2): calcd. C 14.16, H 3.17, N 22.01; found C 13.9, H 3.2, N 21.8. IR (KBr): $\tilde{v}$ = 2190 [υ(CN)] cm^{-1}. ^1H NMR (300 MHz, D_2O): δ = 2.63 (s, CH_2-Pd_1), 2.75 (s, CH_2-Pd_2) ppm.

$\{[Pt(en)(CN)]_4\}(NO_3)_4$ (5): To a solution of $[enPt(H_2O)_2](NO_3)_2$ obtained by stirring $enPtCl_2$ (340 mg, 1 mmol) and $AgNO_3$ (340 mg, 2 mmol) in water (30 mL) for 2 h at 80 °C, followed by filtration of AgCl, was added freshly prepared $enPt(CN)_2$ (1 mmol in 50 mL water). The mixture was stirred at room temp. for 24 h and the volume of the solution was reduced to 5 mL. The product crystallized within 2–3 weeks at room temp. The yield was 571 mg (43%). $C_{12}H_{32}N_{16}O_{12}Pt_4$ (1372.8): calcd. C 10.5, H 2.35, N 16.33; found C 10.3, H 2.5, N 16.3. IR (KBr): $\tilde{v}$ = 2192 [υ(CN)] cm^{-1}. ^1H NMR (300 MHz, D_2O): δ = 2.54 (s, CH_2-Pt_1), 2.71 (s, CH_2-Pt_2) ppm.

$[Pd_4(bpy)_2(en)_2(CN)_4](NO_3)_4\cdot 2H_2O$ (6): For the preparation of **6**, two solutions, A and B, were prepared and subsequently mixed: (A): $Pd(bpy)Cl_2$ (167.5 mg, 0.5 mmol) was suspended in MeOH (30 mL) and stirred at 45 °C for 1 d with $AgNO_3$ (170 mg, 1 mmol). AgCl was removed by filtration. (B): $Pd(en)Cl_2$ (118.5 mg, 0.5 mmol) and $AgNO_3$ (170 mg, 1 mmol) were stirred in MeOH (30 mL) at room temp. overnight and then filtered from AgCl. The two solutions (A) and (B) were then mixed and stirred at room temp. for 1 d. The white precipitate was filtered and washed with MeOH. The yield was: 63%. $C_{14}H_{16}N_8O_6Pd_6\cdot 2H_2O$: calcd. C 26.22, H 3.14, N 17.48; found C 26.3, H 3.1, N 17.5. IR (KBr): $\tilde{v}$ = 2190 [υ(CN)] cm^{-1}.

$[Pd(bpy)(en)](SO_4)\cdot 3H_2O$ (7): 7 was obtained as described for **6** using as solvent H_2O (80 mL for each step) instead of MeOH. $[Pd(bpy)(en)](SO_4)\cdot 3H_2O$ crystallized in form of colorless blocks in 11% yield. $C_{12}H_{16}N_4O_4PdS\cdot 3H_2O$: calcd. C 30.48, H 4.69, N 11.85; found C 30.0, H 4.7, N 11.9. ^1H NMR (400 MHz, D_2O): δ = 3.00 (s, CH_2), 7.73 (ddd, 2 H, H_5), 8.26–8.40 (m, 6 H, H_3, H_4 and H_6) ppm.

$[1\text{-}MeC\cdot 1\text{-}MeCH][PdI_2(CN)(1\text{-}MeC)]\cdot 2H_2O$ (8): 8 was obtained when trying to cocrystallize $[Pd(en)(CN)]_4(NO_3)_4$ (**4**) with [1-MeC]I. The product was obtained in form of orange crystals within 2 d at room temp. $C_{16}H_{22}I_2N_{10}O_3Pd\cdot H_2O$: calcd. C 24.62, H 3.10, N 17.94; found C 25.0, H 3.6, N 18.0.

X-ray Crystal Structure Determination: Crystal structures **1**, **3**, **4**, **5**, **5a**, **7**, and **8** were determined with a Xcalibur diffractometer [graphite mono-chromated Mo-K_α radiation (0.71073 Å)]. Data reduction was done with the CrysAlisPro software.[27] The structures were solved by direct methods and full-matrix least-squares refined on F^2 using SHELXL-97 and WinGX software.[28,29] All non-hydrogen atoms were refined anisotropically, whereas hydrogen atoms were positioned geometrically and refined with isotropic displacement parameters according to the riding model.

CCDC-798819 (for **1**), -798820 (for **3**), -798821 (for **4**), -798822 (for **5**), -798823 (for **5a**), -798824 (for **7**), -798825 (for **8**) contain the supplementary crystallographic data for this paper. These data can be obtained free of charge from The Cambridge Crystallographic Data Centre via www.ccdc.cam.ac.uk/data_request/cif.

Crystal Data for $Pd(en)(CN)_2$ (1): $[C_4H_8N_4Pd]$, orthorhombic, $P2_12_12_1$, a = 6.8885(2) Å, b = 9.3234(3) Å, c = 10.9874(3) Å, Z = 4, fw = 218.54 g mol^{-1}, V = 705.66(4) Å^3, $D_{calcd.}$ = 2.057 Mg m^{-3}, μ = 2.545 mm^{-1}, 10564 reflections collected, 1780 unique (R_{int} = 0.0388), $R_1(F_o)$ = 0.0179 [$I > 2\sigma(I)$], wR_2 (F_o^2) = 0.0362 (all data), GOF = 1.011.

$[Pt(en)_2][Pt(CN)_4]$ (3): $[C_8H_{16}N_8Pt_2]$, monoclinic, $P2_1/c$, a = 8.5969(6) Å, b = 13.2140(10) Å, c = 14.2944(10) Å, β = 123.782(5)°, Z = 4, fw = 614.47 g mol^{-1}, V = 1349.67(17) Å^3, $D_{calcd.}$ = 3.024 Mg m^{-3}, μ = 20.704 mm^{-1}, 9736 reflections collected, 3004 unique (R_{int} = 0.0585), $R_1(F_o)$ = 0.0977 [$I > 2\sigma(I)$], wR_2 (F_o^2) = 0.2434 (all data), GOF = 1.090.

$[Pd(en)(CN)]_4(NO_3)_4\cdot 3H_2O$ (4): $[C_{12}H_{38}N_{16}O_{15}Pd_4]$, triclinic, $P\bar{1}$, a = 7.0948(3) Å, b = 10.4874(6) Å, c = 11.9782(6) Å, α = 92.119(4)°, β = 97.420(4)°, γ = 104.373(4)°, Z = 1, fw = 1072.18 g mol^{-1}, V = 853.91(7) Å^3, $D_{calcd.}$ = 2.085 Mg m^{-3}, μ = 2.155 mm^{-1}, 8078 reflections collected, 3551 unique (R_{int} = 0.0239), $R_1(F_o)$ = 0.0497 [$I > 2\sigma(I)$], wR_2 (F_o^2) = 0.1471 (all data), GOF = 1.040.

$[Pt(en)(CN)]_4(NO_3)_4\cdot 4H_2O$ (5): $[C_{12}H_{40}N_{16}O_{16}Pt_4]$, triclinic, $P\bar{1}$, a = 7.9050(5) Å, b = 8.0482(5) Å, c = 13.7847(6) Å, α = 98.550(5)°, β = 91.609(4)°, γ = 100.865(6)°, Z = 1, fw = 1444.96 g mol^{-1}, V = 850.28(8) Å^3, $D_{calcd.}$ = 2.822 Mg m^{-3}, μ = 16.488 mm^{-1}, 8904 reflections collected, 3796 unique (R_{int} = 0.0511), $R_1(F_o)$ = 0.0445 [$I > 2\sigma(I)$], wR_2 (F_o^2) = 0.0838 (all data), GOF = 0.946.

$\{[Pt(en)(CN)]_4\}(C_8H_4O_4)\cdot 10H_2O$ (5a): $[C_{28}H_{60}N_{12}O_{18}Pt_4]$, triclinic, $P\bar{1}$, a = 7.0391(4) Å, b = 13.0244(8) Å, c = 13.1857(8) Å, α = 75.773(5)°, β = 79.050(5)°, γ = 84.799(5)°, Z = 1, fw = 1633.24 g mol^{-1}, V = 1149.21(12) Å^3, $D_{calcd.}$ = 2.360 Mg m^{-3}, μ = 12.215 mm^{-1}, 9951 reflections collected, 5225 unique (R_{int} = 0.0492), $R_1(F_o)$ = 0.0589 [$I > 2\sigma(I)$], wR_2 (F_o^2) = 0.1393 (all data), GOF = 0.940.

$[Pd(en)(2,2'\text{-}bipy)](SO_4)\cdot 3H_2O$ (7): $[C_{12}H_{22}N_4O_7PdS]$, monoclinic, $P2_1/c$, a = 12.7668(10) Å, b = 8.4206(8) Å, c = 19.7814(19) Å, β = 128.463(6)°, Z = 4, fw = 472.8 g mol^{-1}, V = 1665.1(3) Å^3, $D_{calcd.}$ = 1.886 Mg m^{-3}, μ = 1.285 mm^{-1}, 7527 reflections collected, 3792 unique (R_{int} = 0.0443), $R_1(F_o)$ = 0.0792 [$I > 2\sigma(I)$], wR_2 (F_o^2) = 0.1699 (all data), GOF = 1.120.

$[1\text{-}MeC\cdot 1\text{-}MeCH][PdI_2(CN)(1\text{-}MeC)]\cdot 2H_2O$ (8): $[C_{16}H_{26}I_2N_{10}O_5Pd]$, triclinic, $P\bar{1}$, a = 7.4344(3) Å, b = 9.9380(4) Å, c = 18.7338(8) Å, α = 81.029(4) °, β = 86.096(4)°, γ = 69.151(4)°, Z = 2, fw = 798.67 g mol^{-1}, V = 1277.54(9) Å^3, $D_{calcd.}$ = 2.076 Mg m^{-3}, μ = 3.190 mm^{-1}, 12647 reflections collected, 5756 unique (R_{int} = 0.0437), $R_1(F_o)$ = 0.0336 [$I > 2\sigma(I)$], wR_2 (F_o^2) = 0.0457 (all data), GOF = 0.959.

Supporting Information (see footnote on the first page of this article): Selected bond lengths and angles for **1**, **3**, **4**, **5**, **5a**, **7**, and **8**; crystal structure of **3** with atom numbering scheme, and crystal packing of **3** indicating extensive intermolecular hydrogen bonding; view of the cation of **4**; packing arrangement of **5a** in the crystal; chemical shifts of **5** upon addition of 1-MeC, 1-MeUH and 9-EtA.

Acknowledgments

This work was supported by the Deutsche Forschungsgemeinschaft (DFG) and the "International Max-Planck Research School of Chemical Biology" (Dortmund) (fellowship to A. G.).

---

[1] W. P. Fehlhammer, M. Fritz, *Chem. Rev.* **1993**, *93*, 1243–1280.

[2] See, e.g a) S.-W. Liang, M.-X. Li, M. Shao, Z.-X. Miao, *Inorg. Chem.* **2006**, *45*, 1312–1314; b) E. Chelebaeva, J. Larionova, Y. Guari, R. A. S. Ferreira, L. D. Carlos, F. A. Almeida Paz, A. Trifonov, C. Guerin, *Inorg. Chem.* **2009**, *48*, 5983–5995; c) H.-R. Wen, Y.-Z. Tang, C.-M. Liu, J.-L. Chen, C.-L. Yu, *Inorg. Chem.* **2009**, *48*, 10177–10185; d) G. Agusti, M. C. Munoz, A. B. Gaspar, J. A. Real, *Inorg. Chem.* **2009**, *48*, 3371–3381; e) Y. Jin, Y. Qi, S. R. Batten, P. Cao, W. Chen, Y. Che, J. Zheng, *Inorg. Chim. Acta* **2009**, *362*, 3395–3400.

[3] See, e.g a) D. G. Fu, J. Chen, X. S. Tan, L. J. Jiang, G. X. Wang, P. J. Zheng, W. X. Tang, *Inorg. Chem.* **1997**, *36*, 220–225; b) H. Oshio, H. Onodera, O. Tamada, H. Mizutani, T. Hikichi, T. Ito, *Chem. Eur. J.* **2000**, *6*, 2523–2530; c) H. Oshio, M. Yamamoto, T. Ito, *Inorg. Chem.* **2002**, *41*, 5817–5820; d) H. Oshio, H. Onodera, T. Ito, *Chem. Eur. J.* **2003**, *9*, 3946–3950; e) L. Jiang, X.-L. Feng, T.-B. Lu, S. Gao, *Inorg. Chem.* **2006**, *45*, 5018–5026; f) M. D. Ward, *Dalton Trans.* **2010**, *39*, 8851–8867, and ref. cited therein.

[4] See, for instance: a) K. K. Klausmeyer, S. R. Wilson, T. B. Rauchfuss, *J. Am. Chem. Soc.* **1999**, *121*, 2705–2711; b) P. A. Berseth, J. J. Sokol, M. P. Shores, J. L. Heinrich, J. R. Long, *J. Am. Chem. Soc.* **2000**, *122*, 9655–9662; c) J. Y. Yang, M. P. Shores, J. J. Sokol, J. R. Long, *Inorg. Chem.* **2003**, *42*, 1403–1419; d) M. L. Kuhlman, T. B. Rauchfuss, *J. Am. Chem. Soc.* **2003**, *125*, 10084–10092; e) C. P. Berlinguette, J. R. Galan-Mascaros, K. R. Dunbar, *Inorg. Chem.* **2003**, *42*, 3416–3422.

[5] See, for instance: a) E. Gil Bardaji, E. Freisinger, B. Costisella, C. A. Schalley, W. Brüning, M. Sabat, B. Lippert, *Chem. Eur. J.* **2007**, *13*, 6019–6039; b) M. Willermann, C. Mulcahy, R. K. O. Sigel, M. M. Cerda, E. Freisinger, P. J. Sanz Miguel, M. Roitzsch, B. Lippert, *Inorg. Chem.* **2006**, *45*, 2093–2099; c) J. A. R. Navarro, B. Lippert, *Coord. Chem. Rev.* **2001**, *222*, 219–250, and ref. cited therein.

[6] a) M. Roitzsch, B. Lippert, *Angew. Chem.* **2006**, *118*, 153–156; *Angew. Chem. Int. Ed.* **2006**, *45*, 147–150, and ref. cited therein; b) K. Suntharalingam, D. Gupta, P. J. Sanz Miguel, B. Lippert, R. Vilar, *Chem. Eur. J.* **2010**, *16*, 3613–3616.

[7] For various articles, see: *Quadruplex Nucleic Acids* (Eds.: S. Neidle, S. Balasubramanian), RSC Publishing, Royal Society of Chemistry, Cambridge, **2006**.

[8] See, for instance: a) A. Arola, R. Vilar, *Curr. Top. Med. Chem.* **2008**, *8*, 1405–1415; b) S. M. Haider, S. Neidle, *Biochemistry Soc. Trans.* **2009**, *37*, 583–588; c) M. Gunaratnam, S. Swank, S. M. Haider, K. Galesa, A. P. Reszka, M. Beltran, F. Cuenca, J. A. Fletcher, S. Neidle, *J. Med. Chem.* **2009**, *52*, 3774–3783; d) L. Guittat, P. Alberti, D. Gomez, A. De Cian, G. Pennarun, T. Lemarteleur, C. Belmokhtar, R. Paterski, H. Morjani, C. Trentesaux, E. Mandine, F. Boussin, P. Mailliet, L. Lacroix, J.-F. Riou, J.-L. Mergny, *Cytotechnology* **2004**, *45*, 75–90.

[9] See, for instance: a) K. M. Rahman, A. P. Reszka, M. Gunaratnam, S. M. Haider, P. W. Howard, K. R. Fox, S. Neidle, D. E. Thurston, *Chem. Commun.* **2009**, 4097–4099; b) M. Read, R. J. Harrison, B. Romagnoli, F. A. Tanious, S. H. Gowan, A. P. Reszka, W. D. Wilson, L. R. Kelland, S. Neidle, *Proc. Natl. Acad. Sci. USA* **2001**, *98*, 4844–4849; c) R. T. Wheelhouse, D. Sun, H. Han, F. X. Han, L. H. Hurley, *J. Am. Chem. Soc.* **1998**, *120*, 3261–3262.

[10] See, for instance: a) F. X. Han, R. T. Wheelhouse, L. H. Hurley, *J. Am. Chem. Soc.* **1999**, *121*, 3561–3570; b) A. Arola-Arnal, J. Benet-Buchholz, S. Neidle, R. Vilar, *Inorg. Chem.* **2008**, *47*, 11910–11919; c) L. Ren, A. Zhang, J. Huang, P. Wang, X. Weng, L. Zhang, F. Liang, Z. Tan, X. Zhou, *ChemBioChem* **2007**, *8*, 775–780; d) D. P. N. Goncalves, R. Rodriguez, S. Balasubramanian, J. K. M. Sanders, *Chem. Commun.* **2006**, 4685–4687.

[11] F. Stocco, G. C. Stocco, W. M. Scovell, S. Tobias, *Inorg. Chem.* **1971**, *10*, 2639–2646.

[12] See, for instance: a) S.-W. Lai, K.-K. Cheung, M. C.-W. Chan, C.-M. Che, *Angew. Chem.* **1998**, *110*, 193–195; *Angew. Chem. Int. Ed.* **1998**, *37*, 182–184; b) J. Forniés, J. Gómez, E. Lalinde, M. T. Moreno, *Chem. Eur. J.* **2004**, *10*, 888–898; c) I. Ara, N. Chaouche, J. Forniés, C. Fortuño, A. Kribii, A. Martin, *Eur. J. Inorg. Chem.* **2005**, 3894–3901.

[13] a) J. A. Daves, F. R. Hartley, S. G. Murray, M. A. Pierce-Butler, *J. Chem. Soc., Dalton Trans.* **1983**, 1305–1308; b) E. Zangrando, M. Casanova, E. Alessio, *Chem. Rev.* **2008**, *108*, 4975–5013.

[14] a) A. Khutia, P. J. Sanz Miguel, B. Lippert, *Chem. Eur. J.*, manuscript accepted (chem.201002722); b) A. Khutia, P. J. Sanz Miguel, B. Lippert, *Chem. Eur. J.*, manuscript accepted (chem.201002722).

[15] K. Nakamoto, *Infrared and Raman Spectra of Inorganic and Coordinarion Compounds*, John Wiley & Sons, Inc., Hoboken, New Jersey, **2009**.

[16] a) G. Magnus, *Ann. Phys. Chem.* **1828**, *14*, 239–242; b) M. Atoji, J. W. Richardson, R. E. Rundle, *J. Am. Chem. Soc.* **1957**, *79*, 3017–3020.

[17] a) T. G. Appleton, H. C. Clark, L. E. Manzer, *Coord. Chem. Rev.* **1973**, *10*, 335–422; b) G. Raudaschl, B. Lippert, *Inorg. Chim. Acta* **1983**, *80*, L49–L53.

[18] R. Tribolet, H. Sigel, *Biophys. Chem.* **1987**, *27*, 119–130.

[19] See, for instance: B. Lippert, *Coord. Chem. Rev.* **2000**, *200–202*, 487–516.

[20] P. J. Sanz Miguel, P. Lax, M. Willermann, B. Lippert, *Inorg. Chim. Acta* **2004**, *357*, 4552–4561.

[21] See, for instance: a) T. J. Kistenmacher, M. Rossi, L. G. Marzilli, *Biopolymers* **1978**, *17*, 2581–2585; b) T. J. Kistenmacher, M. Rossi, C. C. Chiang, J. P. Caradonna, L. G. Marzilli, *Adv. Mol. Relaxation Interact. Processes* **1980**, *17*, 113–127; c) A. Schimanski, E. Freisinger, A. Erxleben, B. Lippert, *Inorg. Chim. Acta* **1998**, *283*, 223–232; d) J. Müller, E. Freisinger, *Acta Crystallogr., Sect. E* **2005**, *61*, o320–o322.

[22] S. C. Dhara, *Indian J. Chem.* **1970**, *8*, 193–194.

[23] G. B. Kauffman, D. O. Cowan, *Inorg. Synth.* **1963**, *7*, 239–245.

[24] H. T. Kistenmacher, M. Rossi, J. P. Caradonna, L. G. Marzilli, *Adv. Mol. Relax. Interact. Processes* **1979**, *15*, 119–133.

[25] W. Micklitz, B. Lippert, H. Schöllhorn, H. Thewalt, *J. Heterocycl. Chem.* **1989**, *26*, 1499–1500.

[26] J. S. Nowick, J. S. Chen, G. Noronha, *J. Am. Chem. Soc.* **1993**, *115*, 7636–7644.

[27] *CrysAlisPro*, Oxford Diffraction Poland, **2009**.

[28] G. M. Sheldrick, *SHELXS97 and SHELXL97*, University of Göttingen, Germany, **1997**.

[29] L. J. Farrugia, *WinGX*, University of Glasgow, UK, **1998**.

Received: November 19, 2010